Optical properties of a near-$\Sigma 11$ *a* axis tilt grain boundary in α-Al$_2$O$_3$

Shang-Di Mo†, W Y Ching† and R H French‡

† Department of Physics, University of Missouri-Kansas City, Kansas City, Missouri 64110, USA
‡ DuPont Corporation, Central Research, PO Box 80356, Wilmington, Delaware 19880, USA

Abstract. The electronic structure and the optical properties of a near-$\Sigma 11$ grain boundary in α-Al$_2$O$_3$ are studied by means of first-principles calculations based on a structural model constructed by Kenway. Results on the orbital-resolved partial density of states are presented for the grain boundary model and also for a perfect bulk supercell model containing the same number of atoms. An effective-charge calculation indicates an increased ionic character for atoms in the grain boundary region which is attributed to the distorted bonding pattern and a decrease in coordination number. The calculated optical properties show very similar results for the grain boundary model and the bulk supercell model. The electron energy-loss spectra are consistent with the recent experimental data on the near-$\Sigma 11$ grain boundary obtained by spatially resolved valence electron energy-loss spectroscopy.

1. Introduction

It is well known that grain boundaries, which form an important component of the microstructure of polycrystalline materials, have a pervasive influence on a variety of macroscopic properties and phenomena. In α-Al$_2$O$_3$, it has been shown that the sintering, diffusion, deformation behaviour and segregation, as well as chemical and electrical properties, are sensitively dependent on the structure, composition and properties of grain boundaries [1–3]. It is therefore important to study the atomic and electronic structure of the grain boundary (GB) in Al$_2$O$_3$ and to determine the dependence of properties on the GB structures. Of the many types of GBs in Al$_2$O$_3$, the near-$\Sigma 11$ (N$\Sigma 11$) tilt boundary which is formed during the plastic deformation of α-Al$_2$O$_3$ single crystals has been the focus of many recent experimental and theoretical studies [4–8]. Based on high-resolution transmission electron microscopy (HRTEM) and image simulation [4] of the $\Sigma 11$ GB and atomistic pair potential calculation, Kenway has constructed a three-dimensional model for the N$\Sigma 11$ GB [5]. Kenway's model is to date the best description of the N$\Sigma 11$ GB because it closely mimics the HRTEM image diagram and has a very low GB energy [5]. The model contains 72 Al atoms and 108 O atoms and has periodic boundary conditions parallel to the GB region. It has 'free surfaces' in the direction perpendicular to the GB. The 180-atom Kenway model is actually the inner region of a much larger model in the simulation [5]. The 'free surfaces' here correspond to the boundaries of this inner region. Since the Kenway model cannot be made periodic in this direction, calculation of the electronic structure must involve these 'free surfaces'.

We recently investigated the electronic structure of the N$\Sigma 11$ GB in α-Al$_2$O$_3$ based on the Kenway model [7]. We employed the orthogonalized linear combination of atomic orbitals (OLCAO) method [9] in the local density approximation for the electronic structure calculation. The bulk self-consistent potential obtained from the earlier study on the crystalline phase of α-Al$_2$O$_3$ [10] was used for the GB calculation. Parallel calculations on the bulk supercell model containing the same number of O and Al atoms with and without the surface effects were also performed. This extra effort enables us to delineate the effect of the GB in α-Al$_2$O$_3$ by comparing the results with the bulk supercell model calculated in the same fashion. Our results show that the N$\Sigma 11$ GB does not introduce any deep levels into the fundamental gap. Localized states are induced by the GB mainly near the O 2p derived valence band (VB) maximum and the Al 3s derived conduction band (CB) minimum. Calculations of effective charges and bond order were also performed based on the Mulliken scheme [11]. In the GB region, there is an increase in the charge transfer from Al to O and a reduction in the covalent bond formation, due to the lower coordination number of the GB atoms. It was also shown that the calculated partial density of states (PDOS) for the Al atoms in the CB region is in good agreement with the near-edge energy-loss spectrum and the valence electron energy-loss spectrum [6, 8].

In the present paper, we present further results to illuminate the electronic structure of the N$\Sigma 11$ GB in α-Al$_2$O$_3$. In particular, the PDOS values for all atomic orbitals of O and Al are reported. Based on the effective-charge calculation, we shown that the $\Sigma 11$ GB is reasonably charge-neutral electrostatically. Using the

wavefunctions obtained, we extend our calculation to the optical properties and the energy-loss spectrum for the $\Sigma 11$ GB. We then compare our calculated results with the recent quantitative measurement of the electronic structure of bulk α-Al_2O_3 and at the N$\Sigma 11$ GB by spatially resolved electron energy-loss (SREEL) spectroscopy [6, 8]. In the calculation of DOS, effective ionic valence and bond order, a basis set including Al 3d, Al 4s and Al 4p and O 2s and O 2p were used. For the calculation of optical properties, the extended basis set includes O 3s and O 3p orbitals as well in order to improve the accuracy of the CB wavefunctions. The band secular equations were solved at four real k points over the small Brillouin zone (BZ) for the GB model calculation and the resulting eigenvalues and wavefunctions were used for the DOS and optical calculations. The PDOS and the effective charges on each atom were obtained by using the Mulliken scheme [11]. The calculation of optical properties includes the evaluation of all momentum matrix elements for dipole transitions between the occupied VB and the empty CB.
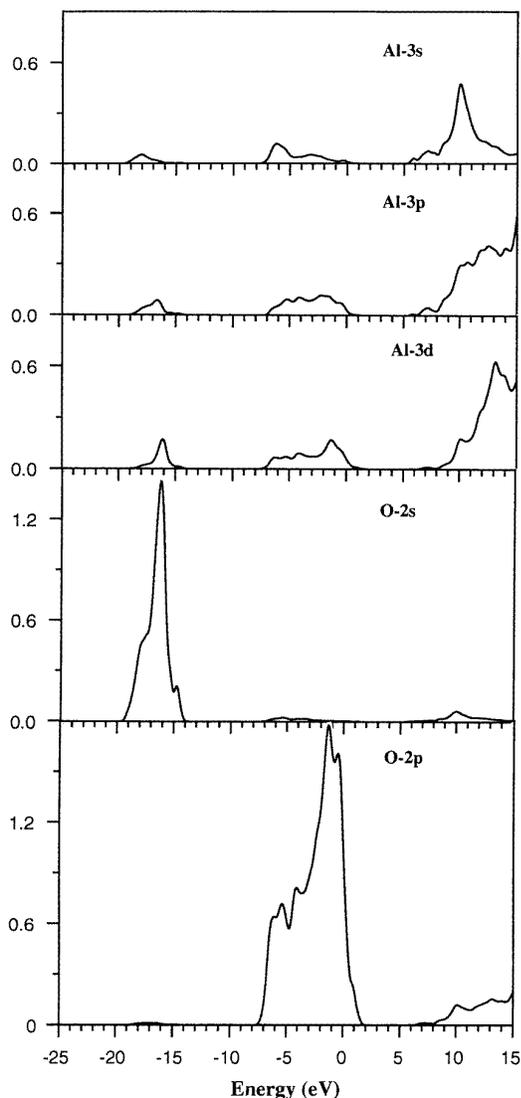
2. Electronic structures

Figures 1 and 2 show the calculated orbital-resolved PDOS for the bulk supercell model and the GB model respectively. As pointed out in the earlier paper [7], the total DOS and PDOS values for the two models have similar features. The similarity in the PDOS values indicates that the GB atoms only weakly influence the overall electronic structure and bonding in α-Al_2O_3. Nevertheless, there are also some differences induced by the GB which can be summarized as follows. (i) There is a significant number of relatively localized states originating from the GB atoms at the top of VB and the upper edge of the O 2s band. This resulted in a larger bandwidth for the O 2s and O 2p bands and a smaller gap between them. (ii) The shape of the CB DOS changes substantially. It is important to analyse the changes in the CB DOS because they can be compared with experimental SREEL spectra. In figure 3, we make a more detailed comparison of the Al 3s, Al 3p and Al 3d PDOS in the CB region. By comparing the results for the bulk supercell and the GB model, we find that, for the GB, there is a 0.5 eV upward shift in the peak position for the Al 3s PDOS and that the Al 3s peak is more broadened. The Al 3p PDOS for the GB has no distinct peak and its distribution extends closer to the gap region. For the Al 3d PDOS, it appears that, for the GB, the general feature is retained except it is more broadened and states at the lower CB are re-distributed, extending more into the gap region. The experimental energy-loss near-edge Al $L_{2,3}$ spectrum [6] shows that the GB introduces additional fine structure. Because the 2p to 3p transitions are dipole-forbidden, the difference in the Al $L_{2,3}$ spectrum is mainly attributed to the changes in the Al 3s and Al 3d states. It reflects the reduced point-group symmetry and also the change in the coordination number of the atoms in the GB region. Our calculated PDOS result is consistent with the experimentally observed changes, as has already been discussed [7].
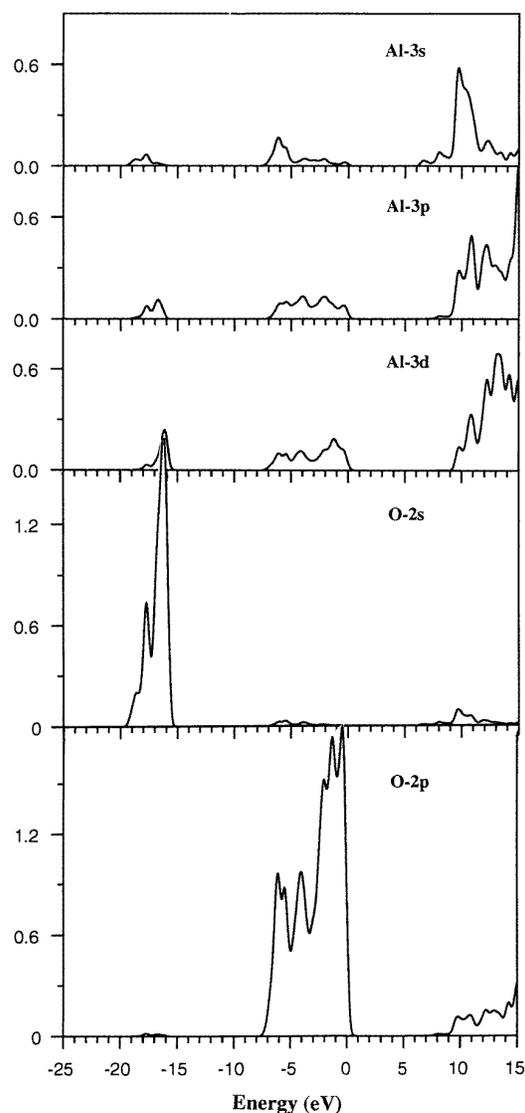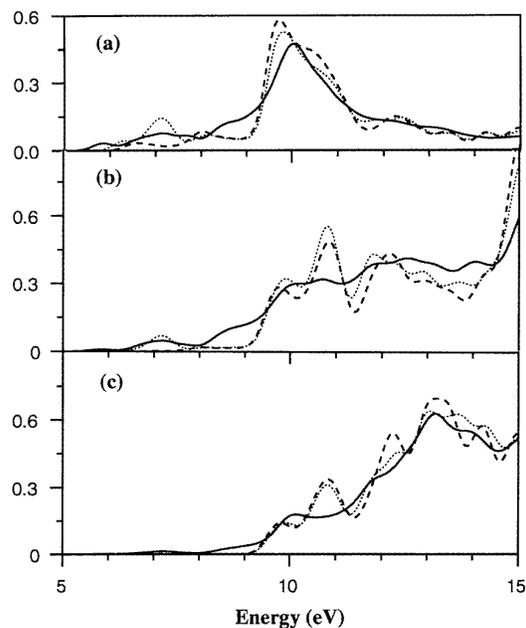
Figure 1. Calculated atom- and orbital-resolved PDOS values for a bulk supercell model of α-Al_2O_3 (see [7] for the details of the model).

To have a better understanding of the effect of the GB in α-Al_2O_3, it is important to have a quantitative evaluation of the charge transfer and the strength of bonding for the GB atoms and to correlate it with the local geometric structure. The ionic valence (defined as the number of outer valence electrons minus the effective charge) indicates the degree of charge transfer, while the bond order (also called the overlap population) represents the strength of the covalent bonding between two neighbouring atoms. In general, a large bond order value means a higher percentage of covalent bonding. In the earlier paper [7], we showed that the undercoordination of the GB atoms led to an increase in the charge transfer and a concomitant decrease in the covalent bonding character. Here, we focus more on some specific GB atoms that are more representative of this general picture. These GB atoms are loosely defined as those atoms which are within 3 Å of the GB line. Their bond lengths and bond angles deviate significantly

Figure 2. The same as figure 1 for the NΣ11 GB model.

Figure 3. A close-up comparison of the conduction band PDOS of Al between the bulk supercell model (broken line), the supercell model with surfaces (dotted line) and the NΣ11 GB model (full line): (*a*) Al 3s, (*b*) Al 3p and (*c*) Al 3d.

from the bulk crystalline values. Figure 4 shows a close-up view of the bonding configurations of the GB atoms in the Kenway model. The thick broken line represents the Σ11 GB line and the short broken lines depict the repeating units of a group of GB atoms that is consistent with the HRTEM picture [4]. We display the calculated ionic valence at each atom and the interatomic distances between the neighbouring atoms. For the bulk supercell model, we obtained an average effective charge of 2.07 for Al and 6.62 for O which give effective ionic valences of +0.93 and −0.62 respectively, as described before [7]. In the GB region, there is a general increase in the effective ionic valence due to the increased charge transfer from Al to O. Among the GB atoms, the largest ionic valences are +1.30 for Al and −0.83 for O for a pair of atoms with a very small separation of 1.75 Å. The smallest ionic valences are +0.72 and −0.59 for Al and O respectively. The coordination numbers and interatomic separations for these two atoms are close to those of the α-Al$_2$O$_3$ bulk structure. In general, a smaller bond length correlates with

larger charge transfer. We have identified a group of four atoms in the GB region (marked by a full circle) among which the largest charge transfer occurs. The ionic valences for the two O atoms are −0.83 and −0.75 and the ionic valences for the two Al atoms are +1.30 and +1.26. These values are much larger than the average ionic valence for the atoms in GB and those in the bulk. The interatomic distances between these four atoms are 1.75, 1.77, 1.77 and 1.76 Å respectively, much smaller than the two typical bond lengths of 1.86 and 197 Å in the bulk α-Al$_2$O$_3$. The bond orders of the four bonds in that region are found to be 0.13, 0.13, 0.15 and 0.15 (shown as numbers in parentheses). They are within the range 0.09–0.17 of average bond order in the other parts of the GB region. The bond order is not only related to the interatomic distances, but to certain extent also to the bond angles.

It is interesting to determine whether the NΣ11 GB in α-Al$_2$O$_3$ is locally charged across the GB line. To this end, we calculated the average ionic valence of the cations and anions on both sides of the GB line which is represented by the thick broken line in figure 4. Because the numbers of Al and O atoms on each side of the GB line in the GB region are not the same, it is necessary to take the average value of the ionic valence for each type of atom. It is found that the left-hand side has average ionic valence +1.01 for Al and −0.68 for O, whereas the corresponding values on the right-hand side are +0.96 and −0.65 respectively. The difference is quite small. This simple analysis seems to suggest that the charge are nearly balanced across the NΣ11 GB in α-Al$_2$O$_3$. It is therefore unlikely that the NΣ11 GB will cause a large amount of impurity segregation. It has to be admitted that this conclusion is based on a rather simplified
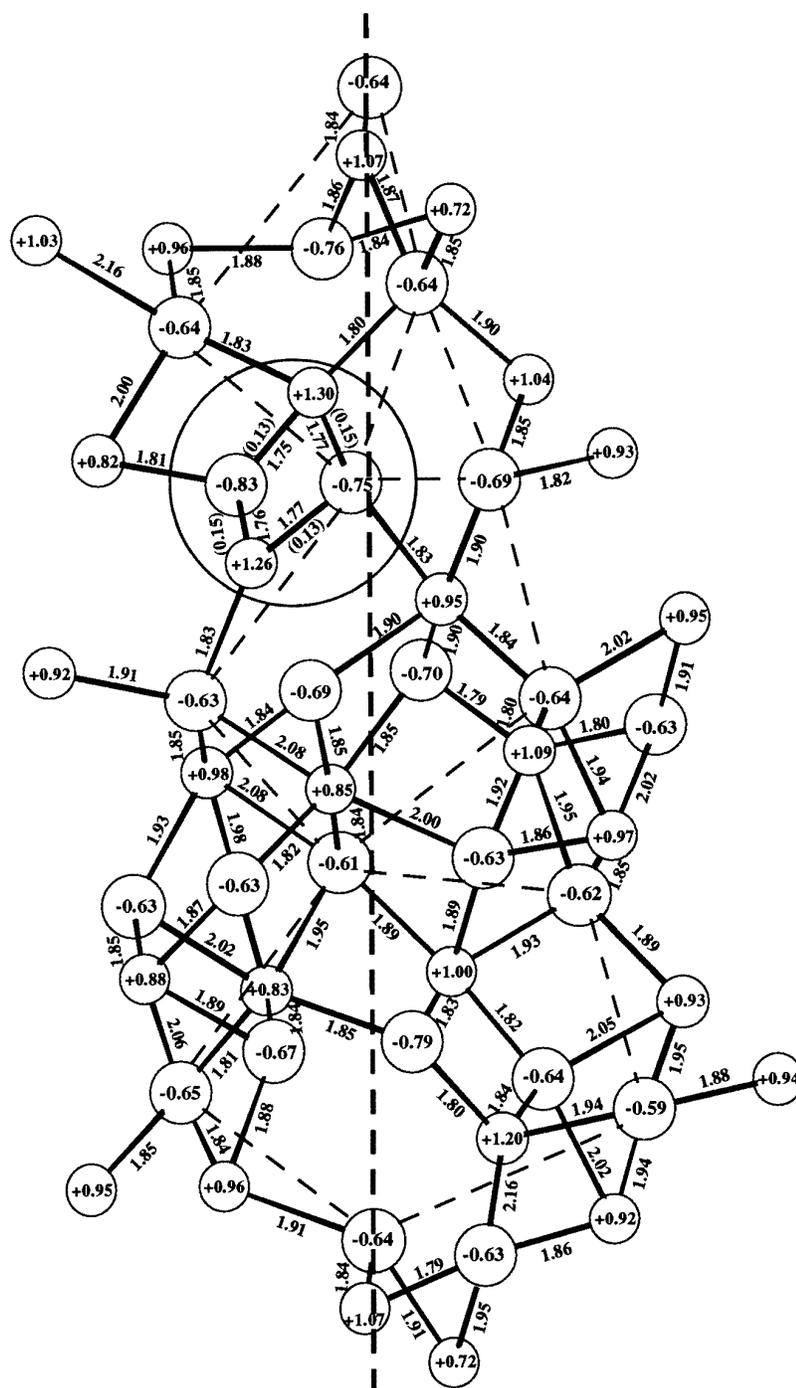
Figure 4. The geometry of the GB atoms in the Kenway model (see [7] for the details of the model). The large circles represent the O atoms and the smaller circles the Al atoms. The numbers within the circles are the calculated ionic valences for the atoms. The numbers between the atoms are the interatomic distances in ångström units. The large circle encloses a group of four atoms with the largest distortions (see the main text). The numbers in the parentheses within the circle show the bond orders between pairs of atoms. The thin broken lines outline the repeating unit of the GB atoms in the NΣ11 GB. The long thick broken line represents the GB line.

model, but it is consistent with the fact that the NΣ11 GB is a low-energy GB in α-Al$_2$O$_3$. More detailed analysis of the space charge distribution requires direct real-space calculation of the charge and potential distributions in the GB region.

3. Optical properties

To obtain further insight on the electronic structure of the NΣ11 GB in α-Al$_2$O$_3$, we calculated the interband optical transitions of the GB represented by the Kenway model.

A parallel calculation concerning the bulk supercell model was also performed for comparison. The interband optical conductivity was calculated according to the expression

$$\sigma(\hbar\omega) = \frac{2\pi e^2}{mE\Omega} \frac{\Omega}{(2\pi)^3} \int dk \sum_{n,l} |\langle \psi_n(k,r)|p|\psi_l(k,r)\rangle|^2$$
$$\times f_l(k)[1 - f_n(k)]\delta[E_n(k) - E_l(k) - \hbar\omega] \quad (1)$$

where $\hbar\omega$ is the photon energy, $f(k)$ is the Fermi distribution function and l and n label the occupied and unoccupied states respectively. Ω is the volume of the model cell. Other optical constants such as the complex dielectric function can be obtained from the interband optical conductivity spectrum [9].

The calculated real and imaginary parts of the dielectric functions and the electron energy-loss spectroscopy (EELS) for the bulk supercell model and the GB model in α-Al_2O_3 are shown in figure 5. Before we comment on the results of figure 5, we must first discuss two correction procedures adapted by us. The first is the elimination of the surface states in the GB calculation. As pointed out before [7], the Kenway model has only two-dimensional periodicity and there are 'free surfaces' in the direction perpendicular to the GB. In evaluation equation (1) for $\sigma(\hbar\omega)$, we eliminated those states whose wavefunctions have a preponderant concentration on the 'surface' atoms and hence were classified as 'surface states' that play no role in the GB. However, since the 'surface states' are distributed mostly near the gap edges, we found that the elimination of the 'surface states' resulted only in a small change in the optical properties near the absorption edge. The second point is that, both in the bulk supercell model and in the GB model calculations, we are dealing with a large complex system of 180 atoms. The wavefunctions of the high CB in the LCAO representation obtained variationally are likely to be less accurate when the dimension of the secular equations becomes huge. This may have resulted in the overestimation of the transition matrix elements in the high-frequency region. The fact that we restricted our calculation of $\sigma(\hbar\omega)$ to only a few k points where the wavefunctions are real may also have contributed to the erosion of accuracy in that region. We have therefore applied a rather arbitrarily designed scaling function to the calculated imaginary part of the dielectric function $\varepsilon_2(\omega)$ for $\hbar\omega > 19$ eV. The scaled $\varepsilon_2(\omega)$ is smoothly joined to the original $\varepsilon_2(\omega)$ at 19 eV but decreases its amplitude as the square of the photon energy. We found that this correction procedure, albeit somewhat arbitrarily, provides us with reasonably consistent results which are shown in figure 5. Our correction procedure is further justified by the fact that we are more concerned with the relative changes in the optical properties of the bulk supercell and the GB models. We believe our results are meaningful since the same computational procedure and the same correction scheme were applied both to the bulk supercell model and the GB model.

Figure 5(a) shows the calculated $\varepsilon_2(\omega)$ curves for the bulk supercell and for the GB models. The result for the supercell model is similar to that of the perfect crystalline calculation [10]. The difference can be attributed to the small k-point resolution in the supercell calculation. Except for the relatively lower height and a flat structure in the range 10–17 eV, the GB model has essentially the same features
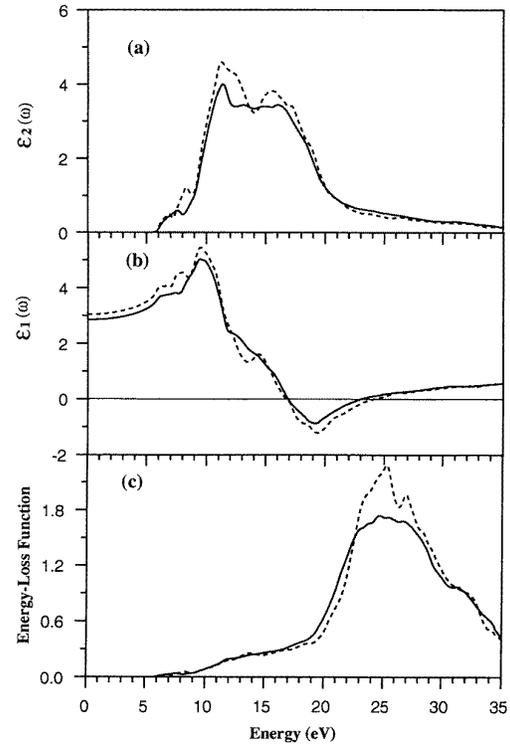
Figure 5. The calculated optical properties for the NΣ11 GB model (full line) and the bulk supercell model (broken line): (a) the imaginary part of dielectric functions, (b) the real part of the dielectric functions and (c) the electron energy-loss functions.

as the bulk supercell model. This resemblance is carried over to the real part of the dielectric function $\varepsilon_1(\omega)$ shown in figure 5(b) obtained by Kramers–Kronig conversion. The static dielectric constant $\varepsilon_1(0)$ is estimated to be 3.05 for the bulk supercell and 2.86 for the GB model, which give the estimated values of the ordinary refractive index of 1.76, and 1.69 respectively. Both values are quite close to the measured value of 1.77 of crystalline α-Al_2O_3 [12]. The reduction in the static dielectric constant for the GB model is the result of a reduction in the mass density in the GB region and the accompanied modification of the electronic structure. The EELS obtained from the complex dielectric function are presented in figure 5(c). Both for the GB and for the bulk supercell model, there are plasmon peaks at approximately 25 eV, but the EELS for the GB has a lower peak height and a less compact structure. In the 17–23 eV region within which the EELS rises rapidly, the amplitude for the GB is higher than that of the bulk supercell, with the cross over occuring at about 22.6 eV. However, in the high-frequency region, the EELS is very sensitive to the structures in the complex dielectric function, so absolute accuracy cannot be guaranteed. The above features appear to be in general agreement with the recent experimental spatially resolved energy-loss spectra of the bulk and NΣ11 GB reported by Müllejans *et al* [8]. The experimental data show that the main change appears most prominently in the energy range 14–22 eV on the low-energy side of the bulk plasmon peak. In that region, the single-scattering bulk energy loss function in the GB region is slightly higher

than that obtained from the nearby bulk region. The same data in conjunction with critical point analysis [13] show an increased ionicity for atoms in the GB region.

4. Conclusions

We have calculated the electronic and optical properties of a near-$\Sigma 11$ tilt boundary in α-Al_2O_3 represented by the Kenway model using the first-principles OLCAO method. The calculated PDOS results show that the GB atoms induce states mainly at the edges of the VB, the O 2s band and the CB. The changes in the PDOS in the VB due to the GB are minimal, but there are significant changes in the CB. There is a general increase in the charge transfer from the Al atoms to the O atoms in the GB region. The increase in the effective ionic valence is the result of local distortion of the Al–O coordination and bonding pattern. We also conclude that the N$\Sigma 11$ GB in α-Al_2O_3 is a relatively charge-neutral GB. Our calculated optical properties show the differences in the dielectric and electron energy-loss functions between the bulk α-Al_2O_3 and the α-Al_2O_3 with a N$\Sigma 11$ GB to be rather small, except that the latter has a relatively smaller static dielectric constant and a more broadened peak in the electron energy-loss spectra. These results are consistent with some of the recent experimental measurements on the $\Sigma 11$ GB in α-Al_2O_3. The present study demonstrates the effectiveness of combining first-principles calculations based on realistic structure models and real-space-based spectroscopy in understanding the electronic properties of complex ceramic structures.

Acknowledgment

References

[1] Morrisey K J and Carter C B 1984 Faceted grain boundaries in Al_2O_3 *J. Am. Ceram. Soc.* **67** 291–301
[2] Priester L and Lartigue S 1988 Grain boundaries in fine-grained magnesium-doped alumina *J. Am. Ceram. Soc.* **71** 430–7
[3] Böker A, Brokmeier H G and Bunge H J 1991 Determination of preferred orientation textures in Al_2O_3 ceramics *J. Eur. Ceram. Soc.* 187–94
[4] Höche T, Kenway P R, Kleebe H-J, Rühle M and Morris P A 1994 High resolution transmission electron microscopy studies of a near $\Sigma 11$ grain boundary in α-alumina *J. Am. Ceram. Soc.* **77** 339–48
[5] Kenway P R 1994 Calculated structures and energies of grain boundaries in α-Al_2O_3 *J. Am. Ceram. Soc.* **77** 349–55
[6] Bruley J 1993 Spatially resolved electron energy-loss near-edge structure analysis of a near $\Sigma = 11$ tilt boundary in sapphire *Microsc. Microanal. Microstruct.* **4** 23–39
[7] Shang-Di Mo, Ching W Y and French R H 1996 Electronic properties of a near $\Sigma 11$ *a*-axis tilt grain boundary in α-Al_2O_3 *J. Am. Ceram. Soc.* at press
[8] Müllejans H, Bruley J, French R H and Morris P A 1994 Quantitative electronic structure analysis of α-Al_2O_3 using spatially resolved valence electron energy-loss spectra *Mater. Res. Soc. Symp. Proc.* **332** 169–76
[9] Ching W Y 1990 Theoretical studies of the electronic properties of ceramic materials *J. Am. Ceram. Soc.* **73** 3135–60
[10] Ching W Y and Xu Y N 1994 First-principles calculation of electronic, optical and structural properties of α-Al_2O_3 *J. Am. Ceram. Soc.* **77** 404–11
[11] Mulliken R S 1955 Electron population analysis on LCAO-MO molecular wave functions part I *J. Am. Chem. Soc.* **23** 1833–40l; 1955 part II *J. Am. Chem. Soc.* **23** 1841–6
[12] Zouboulis E S and Grimsditch M 1991 Refractive index and elastic properties of single crystal corundum (α-Al_2O_3) up to 2100 K *J. Appl. Phys.* **70** 772–6
[13] Loughin S 1992 *PhD Thesis* University of Pennsylvania